European Journal of Radiology Open 5 (2018) 177–182

Contents lists available at ScienceDirect

European Journal of Radiology Open

journal homepage: www.elsevier.com/locate/ejro

Case Report

Hilly or mountainous surface: a new CT feature to predict the behavior of pure ground glass nodules?

Andrea Borghesi[a,*], Silvia Michelini[b], Francesco Bertagna[c], Alessandra Scrimieri[a], Stefania Pezzotti[a], Roberto Maroldi[a]

[a] Department of Radiology, University and Spedali Civili of Brescia, Brescia, Italy
[b] Department of Radiology, Fondazione Poliambulanza Istituto Ospedaliero, Brescia, Italy
[c] Nuclear Medicine, University and Spedali Civili of Brescia, Brescia, Italy

ARTICLE INFO

Keywords:
Pure ground glass nodule
Multidetector computed tomography
Computer-assisted image analysis
Quantitative histogram analysis
Follow-up studies

ABSTRACT

Persistent pure ground-glass nodules (pGGNs) typically show an indolent course with very slow growth rates. These slow-growing lesions exhibit different growth patterns regardless of their initial computed tomography (CT) features. Therefore, predicting the aggressive behavior of pGGNs on initial CT remains a diagnostic challenge. The literature reports that computerized analysis and various quantitative features have been tested to improve the risk stratification for pGGNs.

The present article describes the long-term follow-up of two pGGNs with different behavior and introduces, for the first time, a new computerized method of analysis that could be helpful for predicting the future behavior of pGGNs.

1. Introduction

Subsolid nodules (SSNs) manifest on thin-section computed tomography (CT) as focal ground-glass opacities. SSNs are classified as part solid or pure ground glass nodules (pGGNs) according to the presence or absence of a solid component within the lesion [1].

SSNs represent a major diagnostic challenge, as they may be the manifestation of benign and malignant conditions [2]. Malignancies exhibiting ground glass opacity (most often lepidic predominant adenocarcinoma) may remain unchanged for years [2] or show heterogeneous growth patterns with a trend toward a progressive increase in size over time [3].

Persistent SSNs have a high likelihood to represent pre-invasive or invasive adenocarcinomas, particularly part-solid nodules [3–5]. As a result, the updated Fleischner Society guidelines for the management of SSNs, published at the beginning of 2017, recommend a follow-up period for every pGGN or part-solid nodules ≥ 6 mm in diameter [1]. Conversely, for SSNs smaller than 6 mm in diameter, no routine follow-up is recommended [1].

The literature reports that approximately 80% of pGGNs remain unchanged for an extended period [2]; therefore, conservative monitoring of these lesions is justified. However, some authors demonstrate that more than 40% of pGGNs with initial size ≥ 10 mm exhibited growth during follow-up [6]. In addition, other authors reported that persistent pGGNs ≥ 10 mm in diameter should be considered as early adenocarcinomas or their precursors, until proven otherwise [7]. However, it is unclear whether all such lesions should be surgically resected, as most of these lesions will never become clinically evident [2]. As a result, for pGGNs ≥ 10 mm in diameter, a CT follow-up at 6 months and then every 2 years until 5 years is recommended to confirm the absence of growth [1].

Previous studies on the natural history of pGGNs showed that initial size and development of a solid component within the lesion were associated with nodule growth [6,8]. However, a recent study reported that growth was independent from the initial CT features (such as diameter, volume, mean CT attenuation, and mass) and that only the doubling times may provide information on a nodules' aggressiveness [3]. Thus, predicting the aggressive behavior of pGGNs on initial CT remains a complex diagnostic challenge.

The current report describes the natural course of two pGGNs with an initial size close to 10 mm and long-term CT follow-up periods of 7 and 10 years. One pGGN remained stable in size without the development of a solid component, while the other pGGN showed significant growth with the development of an intralesional solid component and bubbly lucencies. The retrospective computerized analysis of these two pGGNs performed on initial thin-section CT images using a three-

* Corresponding author at: Department of Radiology, University and Spedali Civili of Brescia; Piazzale Spedali Civili, 1, I - 25123 Brescia Italy.
E-mail address: andrea.borghesi@unibs.it (A. Borghesi).

https://doi.org/10.1016/j.ejro.2018.09.004
Received 23 May 2018; Accepted 19 September 2018
Available online 02 October 2018

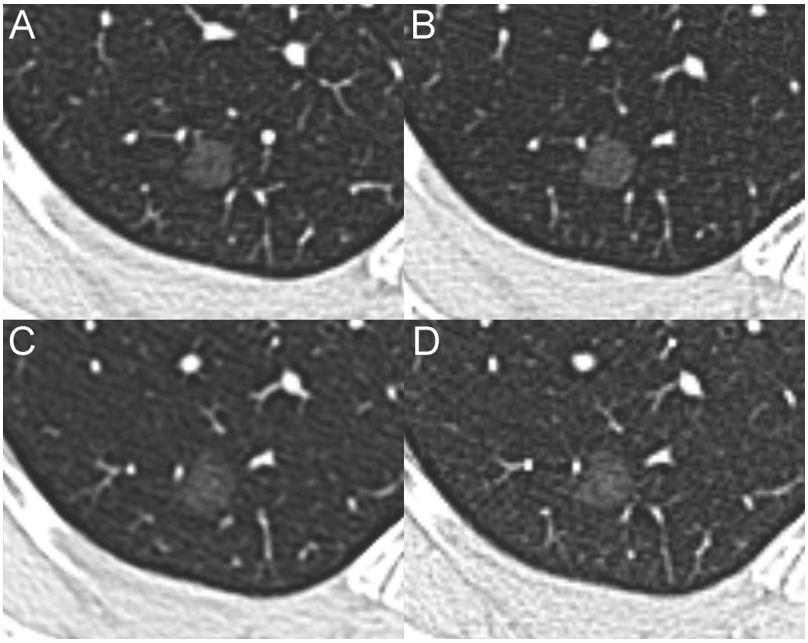

Fig. 1. Serial MDCT scans of the stable pGGN. (A) The baseline MDCT shows a pGGN (mean diameter, 10 mm) in the posterior segment of the right upper lobe. The follow-up CT scans performed at 23 (B), 61 (C) and 83 months (D) reveal the stability of the lesion.

dimensional (3D) surface plot revealed a new distinguishing feature. Therefore, we present this new distinguishing feature and its possible future prospects for differentiating pGGNs ≥ 10 mm that should be followed from those that should be resected.

2. Case report

2.1. Case 1

A 29-year-old Caucasian woman was referred to our radiology department for the monitoring of an endobronchial carcinoid previously located in the right main bronchus and treated with laser.

For this indication, a multidetector computed tomography (MDCT) scan with and without contrast was performed. The patient was asymptomatic and in good health. No sign of persistence or relapse of disease was found on the MDCT scan. However, a pGGN 10 mm in diameter (average of long- and short-axis diameters on the largest cross-sectional area of the lesion) was detected in the posterior segment of the right upper lobe (Fig. 1A). Possible radiologic diagnosis included inflammatory transient lesions and persistent lesions, such as atypical adenomatous hyperplasia and adenocarcinoma in situ. Follow-up CT scans performed 12 and 23 months later revealed the persistence of the nodule without a significant change in the axial diameter (Fig. 1B). Based on the age and history of the patient and the MDCT findings, a long-term follow-up was recommended. Follow-up CT scans at 61 and 83 months showed the stability of the lesion (Fig. 1C and D). Therefore, the patient was reassured, and no further follow-up was recommended.

2.2. Case 2

A 60-year-old Caucasian woman with a previous history of non-Hodgkin lymphoma was referred to our radiology department for the persistence of a consolidation in the left lower lobe.

For this, a MDCT scan without contrast was performed. The MDCT scan showed an irregular consolidation in the left lower lobe (Fig. 2) and a pGGN 12 mm in mean diameter in the anterior segment of the right upper lobe (Fig. 3A). Bronchoscopy and biopsy focused on the left irregular consolidation revealed squamous cell lung cancer. Therefore, a left lower lobectomy was performed with a histological diagnosis of squamous cell lung cancer (pT3N0M0).

For pGGN in the right upper lobe, possible radiologic diagnosis included inflammatory transient lesions and persistent lesions such as atypical adenomatous hyperplasia and adenocarcinoma in situ. A follow-up CT scan performed 12 months later revealed the persistence of pGGN with an initial change in the axial diameters (from 12 mm to 15 mm) (Fig. 3B). No sign of persistence or relapse of disease was found in the left lung. Based on the history of the patient and the MDCT findings, periodic follow-up was suggested. Follow-up CT at 25 and 42 months (Fig. 3C and D) revealed a progressive increase in size of the pGGN and the development of a bubbly lucency within the lesion. The subsequent CT follow-up scans, the last performed at 106 months from baseline, showed a further significant increase in the size of the lesion, numeric and dimensional growth of the bubbly lucencies and development of an intralesional solid component (Fig. 3E). The aggressive behavior of the lesion was considered highly suspicious for a radiological diagnosis of lepidic predominant invasive adenocarcinoma. Therefore, a bronchoscopy with transbronchial biopsy was recommended. The multiple transbronchial biopsies performed within the area of the lesion were negative for neoplastic cells. Despite this result, the lesion was still considered highly suspicious. Based on the comorbidities (chronic HBV-related liver disease, chronic kidney disease stage 3 A, peripheral arterial disease of the lower extremities, Raynaud syndrome) and the clinical status of the patient, surgical treatment was not recommended, and only periodic CT follow-up was suggested. The next CT follow-up scan, performed 120 months after baseline, revealed a significant change in the morphology of the lesion characterized by the collapse of the bubbly lucencies and a further significant increase in the solid component showing peripheral calcifications (Fig. 3F). The PET-CT scan, obtained 1 month later, showed fluorodeoxyglucose (FDG) uptake of the intralesional solid component (SUVmax 4.7) (Fig. 4). No other active lesions in the rest of the body were detected; particularly, non-pathological FDG uptake was observed in hilar or mediastinal lymph nodes. Based on the CT and PET-CT findings and the comorbidities of the patient, stereotactic radiotherapy or radiofrequency ablation was suggested as a valid therapeutic option.

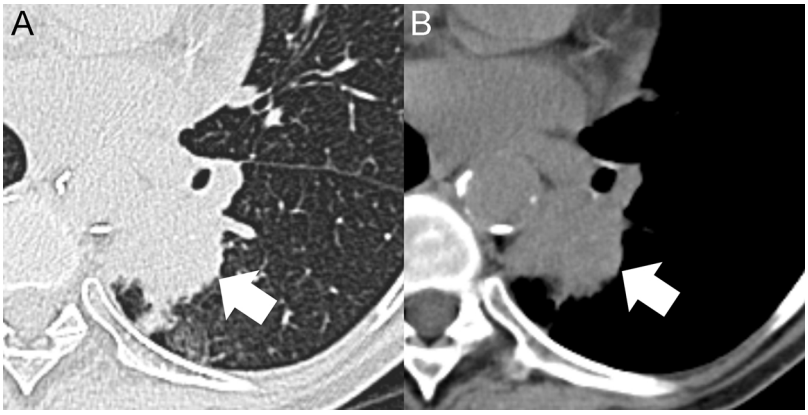

Fig. 2. Axial MDCT images with lung window (A) and mediastinal window (B) show an irregular consolidation in the left lower lobe (*arrows*). The pulmonary lesion was surgically removed with histological diagnosis of squamous cell lung cancer (pT3N0M0).

2.3. Computerized analysis

Considering the similar two-dimensional appearance of the pGGNs at the baseline MDCT and their different behaviors during the long-term follow-up periods, we retrospectively analyzed whether there were any significant differences in the initial CT quantitative features, such as the mean CT attenuation and its standard deviation, volume and mass calculated on the baseline CT scan. These CT features were calculated by applying a 3D semiautomatic software (SAT module, classic version; Terarecon Inc.) on all thin-section axial images. The mass was

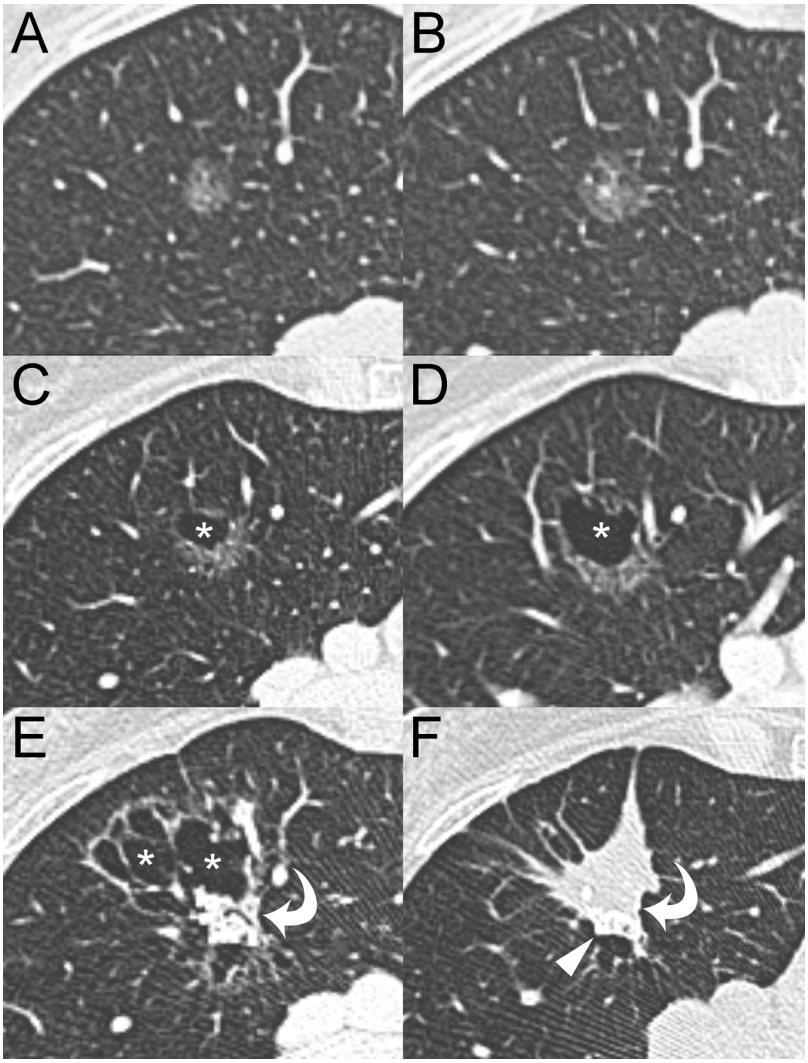

Fig. 3. Serial MDCT scans of the growing pGGN. (A) The baseline MDCT shows a pGGN (mean diameter, 12 mm) in the anterior segment of the right upper lobe. The follow-up CT scans performed at 12 (B), 25 (C), 42 (D), 106 (E) and 120 months (F) demonstrate the stepwise progression of the lesion from pGGN to solid nodule. *Asterisks*, bubbly lucencies; *Curved arrows*, solid component; *Arrowhead*, calcifications.

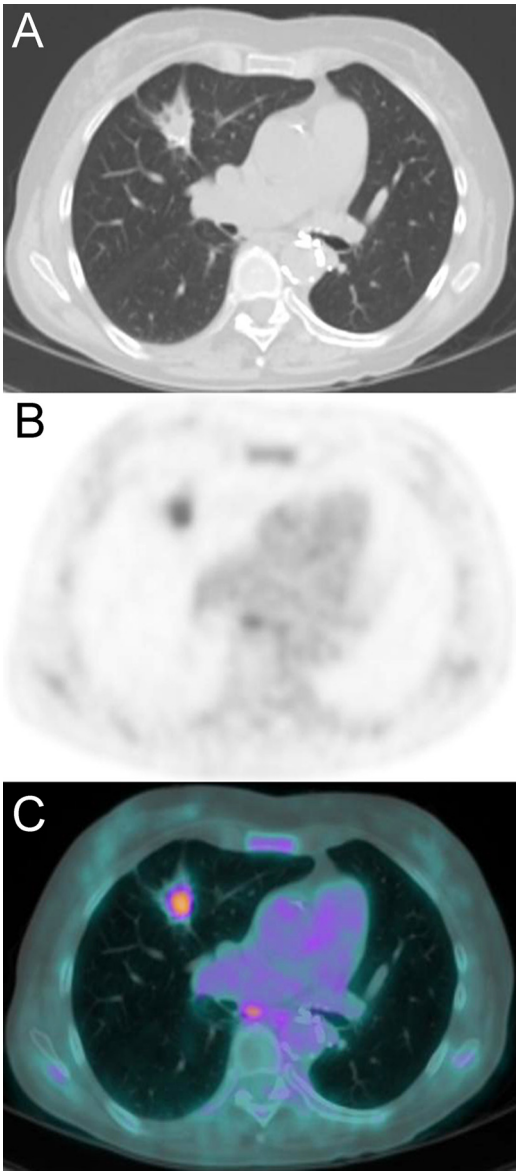

Fig. 4. Axial CT (A), axial PET (B) and axial fused PET/CT (C) images show a pathological FDG uptake within the solid component of the nodule with a SUVmax of 4.7. Note mild inflammatory FDG uptake in a subcarinal lymph node.

calculated by multiplying the volume by the mean nodule density (i.e., mean CT number + 1000) [9].

For both pGGNs, the baseline CT scan was obtained using a 16-detector CT scanner (Somatom Sensation 16, Siemens) with the same acquisition parameters (collimation, 16 × 0.75 mm; beam pitch, 1.0; tube voltage, 120kVp; tube current, 180 mAs) and reconstruction protocol (thin-section 1-mm lung window images with a sharp reconstruction algorithm).

We also investigated whether there were any differences in the distribution of CT attenuation values. For this analysis, the thin-section axial lung window images in DICOM format, which displayed the pGGNs at a magnification of approximately 12×, were saved as 8-bit grayscale files and processed using dedicated software (MATLAB, version R2016b, MathWorks Inc.) applying histogram plots and 3D surface models (named *Mesh*). *Mesh* is a plot that generates a colored, wireframe view of the surface of a matrix data and displays it in 3D view. The color of the *Mesh* plot is determined by Z, so the color is proportional to the surface height, and in the present case, the color and the surface height were proportional to the grayscale value of the pixel.

Table 1
Quantitative computerized analysis of stable and growing pure ground glass nodules at the baseline CT scan.

CT features	Stable pGGN	Growing pGGN
Mean diameter (mm)	10	12
Mean CT attenuation (HU)	−702	−620
SD CT attenuation (HU)	78	154
Volume (mm^3)	354	522
Mass (mg)	105	198

SD, standard deviation; HU, Hounsfield unit; pGGN, pure ground glass nodule.

Before applying the histogram and *Mesh* plots, the pGGNs were segmented manually by outlining the nodule contours on the largest cross-sectional area. Once the segmentation process was completed, the resulting images were processed with the two graphics functions, and then the software automatically generated the histogram and *Mesh* plots. This computerized analysis was performed by an experienced radiologist (with more than 10 years of experience in thoracic imaging).

The CT quantitative features of the stable and growing pGGNs are listed in Table 1.

On the histogram plots, the growing nodule showed a more heterogeneous distribution of grayscale values (Fig. 5D) than did the stable nodule (Fig. 5C). On the *Mesh* plots, the growing nodule presented a more uneven surface with four peaks (red color in Fig. 5B), which looked like a *mountain* (Fig. 5B), whereas the stable nodule showed a more regular surface without peaks, which looked like *a hill* (Fig. 5A).

3. Discussion

Persistent pGGNs typically show an indolent course with very slow growth rates, and consequently, they can be safely managed with annual or biennial CT follow-up [1,10]. These slow-growing lesions exhibit different patterns of growth regardless of their initial CT features [3]. Therefore, appropriate knowledge of the growth patterns of pGGNs is an important issue in lung cancer screening that impacts guidelines for nodule management [1].

Currently, the updated guidelines of the Fleischner Society include some features that increase the risk of aggressive behavior in pGGNs, such as a diameter greater than 10 mm, the presence of bubbly lucencies and the development of solid components [1]. However, these features are hampered by intra- and interobserver variability [11]. Therefore, computerized analysis and various quantitative features have been tested to reduce the subject variability and improve the risk stratification for pGGNs [3,12–16]. In a literature search of the PubMed database, we found a paper published in 2016 in which the computerized analysis and initial CT features (nodule diameter, volume, density, mass and histogram of CT attenuation value) were evaluated to predict the growth of pGGNs [12]. In this study, only the 97.5^{th} percentile on the CT attenuation histogram and the slope of the CT number from the 2.5–97.5^{th} percentiles calculated on the initial CT scan were useful for predicting growth [12]. Another study published in 2014 suggested that a one-dimensional mean CT attenuation value may be helpful in predicting future changes in pGGNs [13].

The present article reports the natural evolution of two persistent pGGNs with different behaviors. The *first case* presents the clinical course of a stable pGGN during a follow-up period of almost 7 years (Fig. 1), whereas the *second case* describes the stepwise progression from pGGN to a solid nodule during a follow-up period of 10 years (Fig. 3).

At baseline CT, the two-dimensional appearance of these two nodules was quite similar; both lesions were pure, and their mean diameter was close to 10 mm. However, computerized analysis revealed that the growing pGGN showed a greater volume, mass and mean CT attenuation (including its standard deviation) than did the stable pGGN

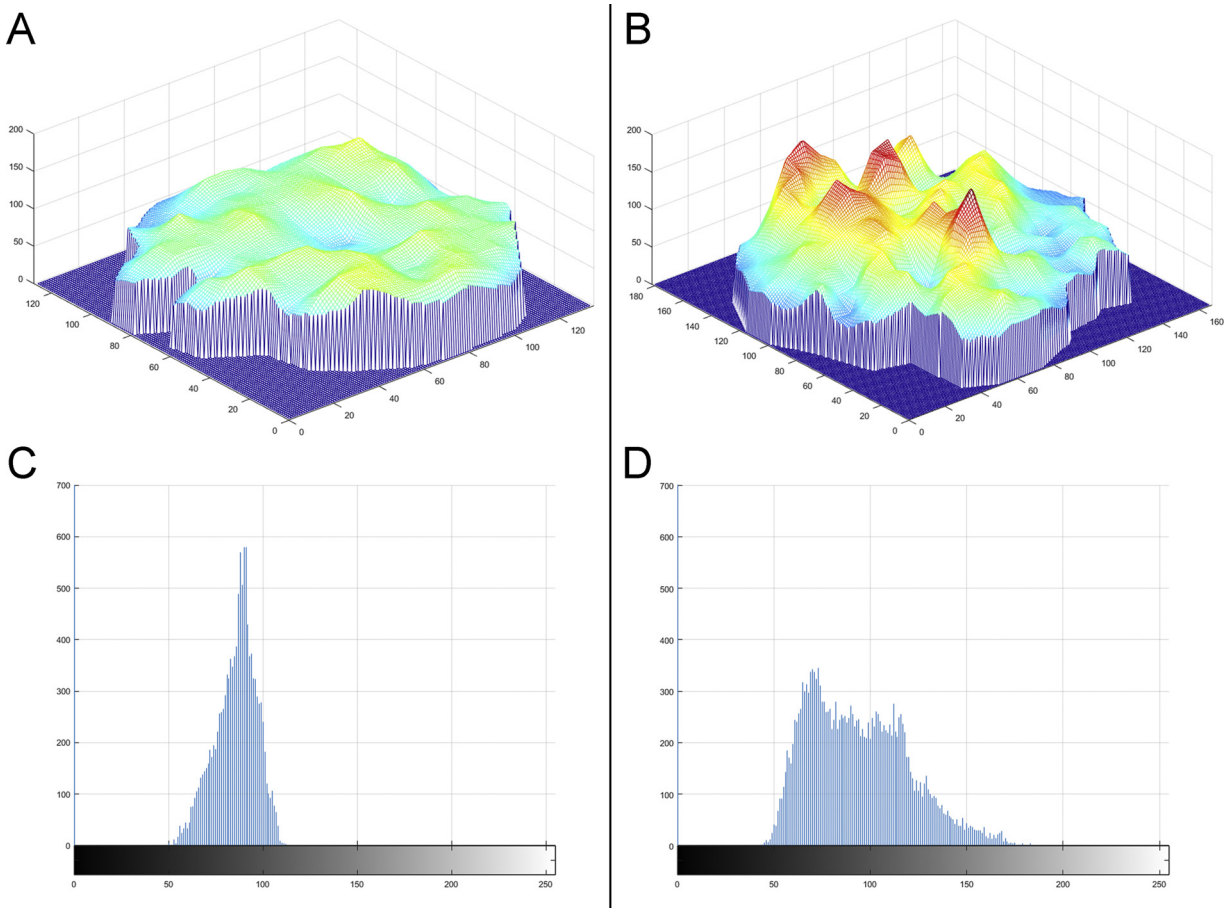

Fig. 5. Mesh plots (A and B) and histogram plots (C and D) demonstrate the different surface morphology (*hilly or mountainous*) and the different distribution of gray values within the largest cross-sectional areas of the stable and the growing pGGNs.

Table 2
Scoring system of the surface morphology for pure ground glass nodules ≥ 10 mm in diameter.

Score	Surface morphology	Peaks	Predicted behavior	First follow-up
1	Hilly	0	Benign	CT at 24 months
2	Hilly predominance	1	Probably benign	CT at 18 months
3	No predominance	2	Indeterminate	CT at 12 months
4	Mountainous predominance	3	Probably aggressive	CT at 9 months
5	Mountainous	4 or more	Aggressive	CT at 6 months

CT, computed tomography.

(Table 1). The main difference between the two pGGNs was related to the standard deviation of the CT attenuation value (twice greater in the growing nodule) (Table 1). The greater standard deviation in the growing nodule reflected the increased heterogeneity of CT numbers within the lesion. This heterogeneity was also shown on the histogram plots and even more so on the *Mesh* plots (Fig. 5B and D).

To the best of our knowledge, there are no published studies in which *Mesh* plots have been tested to assess pGGN heterogeneity. The *Mesh* plot and its 3D surface analysis illustrate the heterogeneity and the distribution of grayscale values within the pixels in a very clear and straight-forward manner. In our *Mesh* plots, the growing pGGN showed a heterogeneous distribution pattern of the grayscale values with four peaks, similar to a *mountainous area* (Fig. 5B), whereas the stable pGGN presented a homogeneous distribution pattern of grayscale values without peaks, similar to a *hilly area* (Fig. 5A). Therefore, we consider the *hilly* or *mountainous* surface morphology on *Mesh* plots to be a new CT feature related to benign or aggressive behavior in pGGNs. In addition, regarding the heterogeneity of pGGNs, the 3D surface analysis obtained with *Mesh* plots is immediate and easier to interpret than is a standard deviation and histogram. Therefore, even those unfamiliar with certain modalities of analysis could understand the nodule heterogeneity distinguishing between a *hilly* or *mountainous* surface morphology.

To quantify the surface morphology obtained using *Mesh* plots, we proposed a dedicated scoring system based on the absence, presence and number of peaks (a possible example is represented in Table 2). The classification of surface morphology and its scoring system could be useful in predicting the behavior of pGGNs ≥ 10 mm in diameter and consequently defining their appropriate intervals for the first CT follow-up.

In conclusion, the present article describes the long-term CT follow-up of two different pGGNs and the first instance in the literature involving the application of *Mesh* plots for predicting pGGN growth. Obviously, we realize that this analysis only included two cases, and the performance of surface morphology (*hilly* or *mountainous*) must be tested in a larger case series. However, we consider this new CT feature

to be very promising in the management of pGGNs, as it may help in the early prediction of their future behavior and consequently in the early identification of surgical and non-surgical nodules.

Conflict of interest

The authors declare no financial or other conflict of interest.

References

[1] H. MacMahon, D.P. Naidich, J.M. Goo, K.S. Lee, A.N.C. Leung, J.R. Mayo, et al., Guidelines for management of incidental pulmonary nodules detected on CT images: from the fleischner society 2017, Radiology (284) (2017) 228–243, https://doi.org/10.1148/radiol.2017161659.

[2] Y. Kobayashi, T. Mitsudomi, Management of ground-glass opacities: should all pulmonary lesions with ground-glass opacity be surgically resected? Transl. Lung Cancer Res. 2 (2013) 354–363.

[3] A. Borghesi, D. Farina, S. Michelini, M. Ferrari, D. Benetti, S. Fisogni, et al., Pulmonary adenocarcinomas presenting as ground-glass opacities on multidetector CT: three-dimensional computer-assisted analysis of growth pattern and doubling time, Diagn. Interv. Radiol. 22 (2016) 525–533.

[4] J.G. Cohen, E. Reymond, M. Lederlin, M. Medici, S. Lantuejoul, F. Laurent, et al., Differentiating pre- and minimally invasive from invasive adenocarcinoma using CT-features in persistent pulmonary part solid nodules in Caucasian patients, Eur. J. Radiol. 84 (2015) 738–744, https://doi.org/10.1016/j.ejrad.2014.12.031.

[5] J.H. Liao, V.B. Amin, M.A. Kadoch, M.B. Beasley, A.H. Jacobi, Subsolid pulmonary nodules: CT-pathologic correlation using the 2011 IASLC/ATS/ERS classification, Clin. Imaging 39 (2015) 344–351, https://doi.org/10.1016/j.clinimag.2014.12.009.

[6] B. Chang, J.H. Hwang, Y.H. Choi, M.P. Chung, H. Kim, O.J. Kwon, et al., Natural history of pure ground-glass opacity lung nodules detected by low-dose CT scan, Chest 143 (2013) 172–178, https://doi.org/10.1378/chest.11-2501.

[7] M. Nakata, H. Saeki, I. Takata, Y. Segawa, H. Mogami, K. Mandai, et al., Focal ground-glass opacity detected by low-dose helical CT, Chest 121 (2002) 1464–1467.

[8] M. Silva, A.A. Bankier, F. Centra, D. Colombi, L. Ampollini, P. Carbognani, et al., Longitudinal evolution of incidentally detected solitary pure ground-glass nodules on CT: relation to clinical metrics, Diagn. Interv. Radiol. 21 (2015) 385–390, https://doi.org/10.5152/dir.2015.14457.

[9] B. de Hoop, H. Gietema, S. van de Vorst, K. Murphy, R.J. van Klaveren, M. Prokop, Pulmonary ground-glass nodules: increase in mass as an early indicator of growth, Radiology 255 (2010) 199–206.

[10] R. Yip, D.F. Yankelevitz, M. Hu, K. Li, D.M. Xu, A. Jirapatnakul, et al., Lung Cancer deaths in the national lung screening trial attributed to nonsolid nodules, Radiology 281 (2016) 589–596.

[11] S.J. van Riel, C.I. Sánchez, A.A. Bankier, D.P. Naidich, J. Verschakelen, E.T. Scholten, et al., Observer variability for classification of pulmonary nodules on low-dose CT images and its effect on nodule management, Radiology 277 (2015) 863–871, https://doi.org/10.1148/radiol.2015142700.

[12] S.H. Bak, H.Y. Lee, J.H. Kim, S.W. Um, O.J. Kwon, J. Han, et al., Quantitative CT scanning analysis of pure ground-glass opacity nodules predicts further CT scanning change, Chest 149 (2016) 180–191, https://doi.org/10.1378/chest.15-0034.

[13] M. Tamura, Y. Shimizu, T. Yamamoto, J. Yoshikawa, Y. Hashizume, Predictive value of one-dimensional mean computed tomography value of ground-glass opacity on high-resolution images for the possibility of future change, J. Thorac. Oncol. 9 (2014) 469–472, https://doi.org/10.1097/JTO.0000000000000117.

[14] Y.S. Song, C.M. Park, S.J. Park, S.M. Lee, Y.K. Jeon, J.M. Goo, Volume and mass doubling time of persistent pulmonary subsolid nodules detected in patients without known malignancy, Radiology 273 (2014) 276–284.

[15] U. Nemec, B.H. Heidinger, K.R. Anderson, M.S. Westmore, P.A. VanderLaan, A.A. Bankier, Software-based risk stratification of pulmonary adenocarcinomas manifesting as pure ground glass nodules on computed tomography, Eur. Radiol. 28 (2018) 235–242, https://doi.org/10.1007/s00330-017-4937-2.

[16] Q. Li, L. Fan, E.T. Cao, Q.C. Li, Y.F. Gu, S.Y. Liu, Quantitative CT analysis of pulmonary pure ground-glass nodule predicts histological invasiveness, Eur. J. Radiol. 89 (2017) 67–71, https://doi.org/10.1016/j.ejrad.2017.01.024.